

Cooling of Ethanol Fermentation Process Using Absorption Chillers*

Felipe Costa Magazoni, Julieta Barbosa Monteiro**, José Miguel Cardemil, Sergio Colle

Laboratory of Energy Conversion Engineering and Energy Technology - LEPTEN
Department of Mechanical Engineering, Federal University of Santa Catarina, 88040-900, Florianópolis, Brazil
E-mail: felipe@lepten.ufsc.br, julieta@lepten.ufsc.br, jose.cardemil@lepten.ufsc.br, colle@emc.ufsc.br

Abstract

Ethanol fermentation is an exothermic process, where the kinetics depends on temperature. This study proposes an alternative cooling system for use in ethanol fermentation using a single-effect water/lithium bromide absorption chiller, powered by waste heat from sugar and ethanol production processes, with a temperature range of 80 to 100 °C. The aim of this study is to model, simulate and analyze the behavior of an absorption refrigeration machine, according to the required cooling capacity of the fermentation system. A comparative analysis with and without the chiller is performed. The introduction of a chiller allowed a reduction in the temperature of the medium of around 1 °C and an increase of around 0.8 % in the fermentation efficiency. Under these conditions less cellular stress occurs and cellular viability is kept at higher levels. The results show that this reduction in temperature can increase the ethanol content of the wine. In the recovery of ethanol, a lower thermal load will be needed at the distillation, with a smaller amount of vinasse produced and consequently the energy efficiency of the plant will increase.

Keywords: Absorption chiller, lithium bromide, cooling, fermentation, ethanol, simulation.

1 Introduction

In industrial ethanol fermentation the yeast cells are submitted to stresses, such as ethanol and sugar concentrations and those originating from environmental factors, operating conditions and physico-chemical factors such as temperature, pH and salts concentration. Of these factors, temperature has the greatest effect on the fermentation kinetics of the process and cell viability (Phisalaphong et al. 2006). Temperature and ethanol can have synergistic effects on the dynamic behavior of the fermentation process. Another consideration with regard to thermal stress is the formation of by-products, such as glycerol and organic acids, mainly succinic and acetic. Studies have shown that the ideal fermentation temperature for increased productivity and maintenance of cell viability is around 32 °C (Aldigui et al. 2004; Phisalaphong et al. 2006).

Currently, the Brazilian ethanol and sugar plants use cooling towers to chill the fermentation process, but these fail to reduce and maintain the temperature of the fermentation medium, since they are dependent on the climate of the region, and this is detrimental to the good performance of the equipment. A small deviation in temperature can affect the kinetic behavior of the fermentation as well as the degree of contamination by bacteria and the development of new *Saccharomyces cerevisiae* strains, as well as wild yeast, and non-*Saccharomyces* species (Torija et al. 2003). There is also a correlation between the ethanol tolerance of yeast cells and fermentation temperature (Aldigui et al. 2004). The temperature also affects the osmotolerance of yeast cells. This factor should be considered especially when cane molasses is used as the substrate. Thus, a cooling system capable of removing the heat released in

order to reduce and keep the fermentation temperature at ideal values is required.

An absorption chiller is thermally driven cooling equipment, which requires small external work. These machines become economically attractive when there is a residual thermal energy source available, such as geothermal energy, solar energy and waste heat from thermal processes (hot exhaust gas discharges, hot water discharges and waste low pressure steam). Single-effect absorption technology provides a peak coefficient of performance approximately 0.8, and it operates with heat input temperatures in the range of 75 to 100 °C (Herold et al. 1996). This study proposes an alternative cooling system for use in ethanol fermentation using a single-effect water/lithium bromide absorption chiller, powered by waste heat from sugar and alcohol production, for example, the contaminated condensate (96 °C) from the sugarcane juice evaporation process, vinasse (80 °C) from distillation and flash saturated steam (100 °C).

The aim of this study is to investigate the behavior of the fermentation process with the introduction of an absorption chiller in the cooling system of the fermentation vats, in an industrial ethanol fermentation process (Usina Cerradinho Açúcar e Alcool S/A).

2 Materials and Methods

2.1 System Description

A schematic diagram of the cooling system for ethanol fermentation is shown in Figure 1. This figure represents the fermentation module of the ethanol industrial process and it consists of the following components: single-effect absorption chiller and fermentation system.

The components of the single-effect water/lithium bromide absorption chiller, shown in region slowroman-

*This paper is an updated version of a paper published in the ECOS'09 proceedings. It is printed here with permission of the authors and organizers

**Corresponding Author

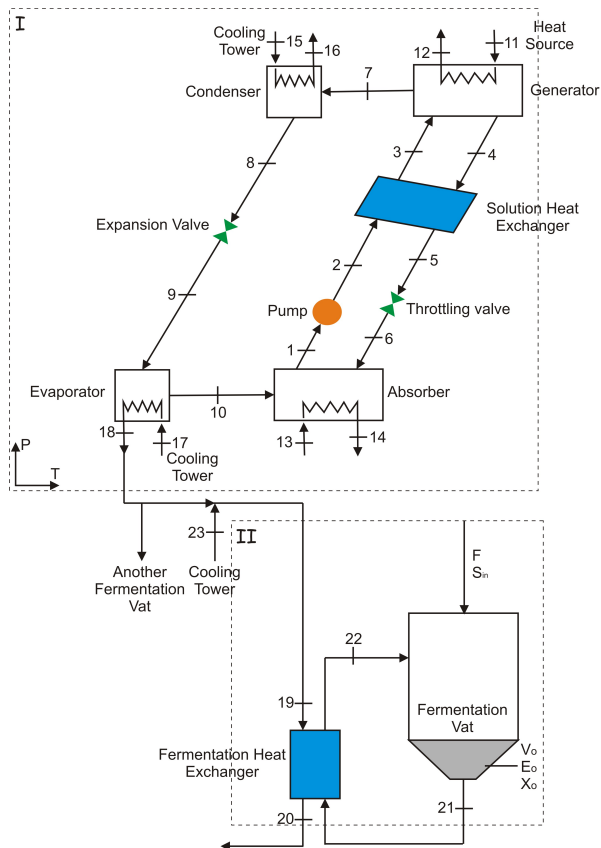


Figure 1. Schematic diagram of the cooling system for ethanol fermentation using a single-effect absorption chiller.

cap@ of Figure 1, are: generator, absorber, condenser, evaporator, solution heat exchanger, solution pump, expansion valve and throttling valve. Firstly, the weak solution of lithium bromide is pumped from the low pressure region in the absorber to the high pressure region in the generator where heat is supplied by the waste heat source (point 11) and the refrigerant water is separated from aqueous lithium bromide solution by evaporation. The superheated steam (point 7) goes through the condenser where it is condensed on the surface of a cooling coil. The saturated water, that leaves the condenser, is throttled through the expansion valve to the lower pressure in the evaporator, where it evaporates by absorbing heat and provides cooling capacity (point 18). The saturated steam from the evaporator (point 10) flows to the absorber where it is absorbed by the strong solution originating from the generator. The mixing process in the absorber is exothermic and needs to reject heat transferring it to the water from the condenser. The weak solution, which leaves the absorber, is pumped to the generator and goes through the solution heat exchanger where it is heated, and the refrigeration process begins again.

One constraint of the single-effect water/lithium bromide absorption chiller is the crystallization of the absorbent (lithium bromide) and the point of the cycle most vulnerable in this regard is the stream entering the absorber (point 6), because of its highly concentrated solution and low temperature.

The absorption chiller has a nominal cooling capacity of 3000 kW and it chills two fermentation vats. The cooling capacity of the absorption chiller was selected

considering the availability of waste heat at the plant. This study only shows the refrigeration of one fermentation vat, thus the mass flow rate of the chilled water from the evaporator is divided into two streams. The volume flow rate and the temperature of some streams in the absorption chiller are shown in Table 1. The configuration of the water loop inlet in the absorption chiller is: condenser (point 15) and evaporator (point 17) use the water from the cooling tower, the absorber uses the water that leaves the condenser (point 16) to reject heat. Usually commercial absorption chillers use inverse configuration (from absorber to condenser) in order to avoid crystallization. As the operation temperature range does not present risk of crystallization, it is reliable to operate under the configuration described above, allowing higher COP (Herold et al. 1996). The generator is heated by the contaminated condensate from the juice evaporation process during sugar production (point 11). The water used to cool the fermentation vat is a mixture of chilled water (point 18) and water from cooling tower (point 23). The simulation of the cooling tower is beyond the scope of this analysis.

Table 1. Volume Flow Rate and Temperature of Some Streams in the Absorption Chiller.

Point	\dot{V} ($\text{m}^3 \text{h}^{-1}$)	T ($^{\circ}\text{C}$)
1	26	–
11	350	96
13	800	T_{16}
15	800	T_{23}
17	450	T_{23}

The ethanol fermentation (region slowromancapii@ in Figure 1) is a biochemical process where the sugars are transformed into alcohol by the industrial yeast *Saccharomyces cerevisiae*. The carbon source used is cane molasses. The fermentation time ranges from 4 to 6 h plus the wait time (1 to 3 h) and there are two fermentation processes per day for each vat. At the end of the fermentation, all sugars have been consumed and the final fermentation product, called wine, has an ethanol concentration of 60 to 90 kg m^{-3} .

The heat released during the ethanol fermentation is removed by means of a plate heat exchanger, where the cold stream (point 19) is provided by both streams, water from the cooling tower (point 23) and from the evaporator of the absorption chiller (point 18). The must from the fermentation vat (point 21) flows to the fermentation heat exchanger with a constant volume flow rate and the flow rate of the cold stream (point 19) is used as a manipulated variable to control the fermentation temperature.

The heat exchangers of the process are in a counter flow arrangement. Plate heat exchangers are used at the solution heat exchanger of the absorption chiller and fermentation heat exchanger, while those of the absorption chiller are shell and tube heat exchangers. The absorption chiller heat exchangers are made of copper while the

fermentation heat exchanger is made of stainless steel AISI 304. The overall thermal conductances UA of heat exchangers are shown in Table 2.

Table 2. Overall Heat Transfer Coefficients of Heat Exchangers.

Component	UA (kWK^{-1})
Generator	165.0
Absorber	297.0
Condenser	198.0
Evaporator	371.3
Solution heat exchanger	31.6
Fermentation heat exchanger	966.4

2.2 Mathematical Modeling

2.2.1 Absorption Chiller The modeling of the absorption chiller is performed based on energy, mass and species balances, considering a quasi-steady state regime (the system moves quickly through a sequence of steady states, even while subjected to varying conditions over time), according to the theoretical fundamentals of Herold et al. (1996).

The mass flow rate balance of the generator is calculated using the expression

$$\dot{m}_3 = \dot{m}_4 + \dot{m}_7 \quad (1)$$

Considering that there is no lithium bromide in the superheated steam (point 7), the lithium bromide balance in the generator is given by

$$\dot{m}_3 \cdot \xi_3 = \dot{m}_4 \cdot \xi_4 \quad (2)$$

where ξ_3 is the lithium bromide mass fraction of the weak solution and ξ_4 is the lithium bromide mass fraction of the strong solution.

The solution pump reaches the steady state flow rate quickly and maintains a constant rate. The expression for the work input of the solution pump is obtained as

$$\dot{W}_p = 100 \cdot \left[\frac{\dot{m}_1 \cdot (P_2 - P_1)}{\eta_p \cdot \rho_1} \right] \quad (3)$$

where η_p is the solution pump efficiency and its value is 72 % and ρ_1 is the density of the aqueous lithium bromide solution at point 1 in Figure 1.

The modeling of the heat exchanger-cycle cooling system of the absorption chiller is carried out using the energy balance and the Logarithmic Mean Temperature Difference (LMTD).

The coefficient of performance (COP) of the refrigeration machine is defined as follows

$$COP = \frac{\dot{Q}_e}{\dot{Q}_g + \dot{W}_p} \quad (4)$$

where \dot{Q}_e is the cooling capacity, \dot{Q}_g is the heat flow input in the generator and \dot{W}_p is the work input of the solution pump.

2.2.2 Fermentation The mathematical model for the ethanol fermentation is an unstructured model and the modeling is performed based on kinetic rate models coupled with mass balance equations for the cell, substrate and ethanol and the energy balance, for an industrial fed-batch fermentation process. It is assumed that the feed is sterile ($X_{in} = 0$).

The global mass balance is described as

$$\frac{dV}{dt} = \dot{F} \quad (5)$$

where \dot{F} is the substrate feed volume flow rate and dV/dt represents the variation in the volume during the fermentation process.

The rate of cell growth is defined as follows

$$\frac{dX}{dt} = \mu \cdot X - \frac{\dot{F} \cdot X}{V} \quad (6)$$

where μ is the specific growth rate and the factor \dot{F}/V is the dilution rate as the feed is added during the fermentation process.

The substrate consumption is modeled by the equation

$$\frac{dS}{dt} = -\frac{\mu \cdot X}{Y_{X/S}} - m_X \cdot X + \frac{\dot{F}}{V} \cdot (S_{in} - S) \quad (7)$$

where $Y_{X/S}$ is the yield factor of the cell based on the substrate consumption and m_X is the maintenance coefficient.

The ethanol formation is written as

$$\frac{dE}{dt} = \frac{Y_{E/S} \cdot \mu \cdot X}{Y_{X/S}} + m_E \cdot X - \frac{\dot{F} \cdot E}{V} \quad (8)$$

where $Y_{E/S}$ represents the yield factor of ethanol based on substrate consumption and m_E is the ethanol production associated with growth.

The variation in fermentation temperature T_{21} during the process is described by Eqn (9) and it is determined through the energy balance of the fermentation system.

$$\begin{aligned} \frac{dT_{21}}{dt} = & \frac{\dot{F}}{V} \cdot (T_{in} - T_{21}) - \frac{\dot{V}_{21}}{V} \cdot (T_{21} - T_{22}) \\ & + \left(\frac{\Delta H_S}{\rho_{in} \cdot C_{p_{in}}} \right) \cdot \left(\frac{\mu \cdot X}{Y_{X/S}} + m_X \cdot X \right) \end{aligned} \quad (9)$$

where ΔH_S is the heat released during the fermentation process and its value is 697.7 kJ per kilogram of substrate consumed (Albers et al. 2002), the inlet temperature T_{in} and the volume flow rate \dot{V}_{21} are shown in Table 4.

In the model shown, the specific growth rate is expressed as a function of limiting substrate concentration S (Monod equation) and of the inhibitory effects of substrate and ethanol concentration (Ghose and Tyagi 1979), as represented by the following equation

$$\mu = \mu_{max} \cdot \left(\frac{S}{K_S + S} \right) \cdot \exp(-K_i \cdot S) \cdot \left(1 - \frac{E}{E_{max}} \right)^n \quad (10)$$

where μ_{max} is the maximum specific growth rate, K_S is the substrate saturation constant, K_i is the substrate

inhibition coefficient, E_{max} is the maximum ethanol concentration at which yeast cell growth is completely inhibited and n is the product inhibition power. Cell inhibition and death are not taken into account in the model due to the dilution effect in the fed-batch mode and the short residence time. This inhibition occurs at high yeast cell concentration, with cell recycling (Jarzebski and Malinowski 1989; Lee et al. 1983). Under industrial conditions, the microorganism is a yeast isolated from the industrial environment and therefore adapted to fermentation stress. In addition, in each fermentation cycle the yeast receives an acid treatment for 2 to 3 h, when nutrients are also supplied.

The parameters used in the model shown above were taken from the literature Atala et al. (2001) and are presented in Table 3. These expressions were determined for the temperature range of 28 to 40 °C, using an industrial yeast *Saccharomyces cerevisiae* (Pedra-2) and cane molasses as the substrate.

Table 3. Kinetic Parameters as a Function of Temperature.

Par.	Expression or Value
μ_{max}	$1.6 \cdot \exp\left(-\frac{41.5}{T_{21}}\right) - 1.3 \cdot 10^4 \cdot \exp\left(-\frac{431.4}{T_{21}}\right)$
E_{max}	$-0.4421 \cdot T_{21}^2 + 26.41 \cdot T_{21} - 279.75$
$Y_{X/S}$	$2.704 \cdot \exp(-0.1225 \cdot T_{21})$
$Y_{E/S}$	$0.6911 \cdot \exp(-0.0139 \cdot T_{21})$
K_i	$1.393 \cdot 10^{-4} \cdot \exp(0.1004 \cdot T_{21})$
K_S	4.1
m_E	0.1
m_X	0.2
n	1.5

The heat flow rate released during the fermentation process \dot{Q}_f is calculated as follows

$$\dot{Q}_f = \Delta H_S \cdot \left[\frac{V_{t-\Delta t} \cdot (S_{t-\Delta t} + S_{in}) - V \cdot S}{3600 \cdot \Delta t} \right] \quad (11)$$

where $S_{t-\Delta t}$ and $V_{t-\Delta t}$ represent the substrate concentration and the working volume of the fermentation vat at time $t - \Delta t$, S and V being the substrate concentration and the working volume at the present time and Δt representing the time difference.

The fermentation heat exchanger is modeled using the Logarithm Mean Temperature Difference (LMTD) method and the energy balance as described in Bejan and Kraus (2003).

The fermentation efficiency may be written as

$$\eta = 100 \cdot \left\{ \frac{E \cdot V - E_0 \cdot V_0}{0.511 \cdot [V \cdot (S_{in} - S) - V_0 \cdot (S_{in} - S_0)]} \right\} \quad (12)$$

where 0.511 is the sugar to ethanol conversion factor based on the theoretical maximum yield.

The ethanol productivity is calculated by the follow-

ing expression

$$\phi_E = \frac{E \cdot V - E_0 \cdot V_0}{V \cdot t} \quad (13)$$

2.3 Simulation

The data collected in a sugar and ethanol production plant (Usina Cerradinho Açúcar e Álcool S/A) are shown in Table 4 and they are used as the initial conditions for the simulation of the industrial fermentation process. For the fermentation, the feed flow rate of the must \dot{F} and the inlet must temperature T_{in} change according to the expressions given in the table. The values for the feed substrate concentration S_{in} , initial cell X_0 and ethanol E_0 concentrations, initial temperature T_0 and initial volume V_0 are shown. The initial time of the refrigeration process is 0.45 h. The water temperature of the cooling tower T_{23} and volume flow rate \dot{V}_{19} were taken during the fermentation process under industrial conditions at the above-mentioned plant and the temperatures vary according to the expression shown.

Table 4. Fermentation Data Collected at Usina Cerradinho Açúcar e Álcool S/A.

Parameter	Expression or Value
\dot{F}	$8.73 \cdot t + 76.29$
S_{in}	200
E_0	34.56
X_0	71.6
T_0	28.37
T_{in}	$0.15 \cdot t + 31.43$
T_{23}	$-0.05 \cdot t^2 + 0.78 \cdot t + 26.03$
V_0	210
\dot{V}_{19}	$-60.0 \cdot t + 1030.1$
\dot{V}_{21}	1000

The simulations were performed using the software Engineering Equation Solver (EES[®], Klein and Alvarado (2008)). The properties of the water are were evaluated with the correlations given by IAPWS (1995). The specific enthalpy of the aqueous lithium bromide solution is was calculated in terms of the solution temperature and lithium bromide mass fraction using the correlation given by ASHRAE (2001). The density and the heat capacity of the aqueous lithium bromide solution are given by the equations of Patterson and Perez-Blanco (1988) and Yuan and Herold (2005), respectively. The correlations of the heat capacity and density of the sugarcane juice used in this work are were calculated by Rao et al. (2009).

3 Results and Discussion

Figure 2 shows the behavior of the fermentation process using only water from cooling tower to chill the vat, where cell X , substrate S and ethanol E concentration profiles are detailed. The fermentation temperature profile (T_{21}) is also presented. The final concentration of ethanol in the simulated fermentation reaches

73.60 kg m⁻³ against a value of 73.41 kg m⁻³ obtained in the industrial fermentation under analysis, representing a difference of 0.3 %, and an ethanol fermentation efficiency of 88.4 %. Considering 8 h of process (fermentation time plus wait time), the ethanol productivity is 7.9 kg m⁻³ h⁻¹. As seen from the figure, the fermentation temperature reaches a maximum of around 36 °C. Thus, the use of water from the cooling tower as the only cooling source is insufficient to keep the fermentation temperature at the ideal value (32 °C), which leads to a lower efficiency.

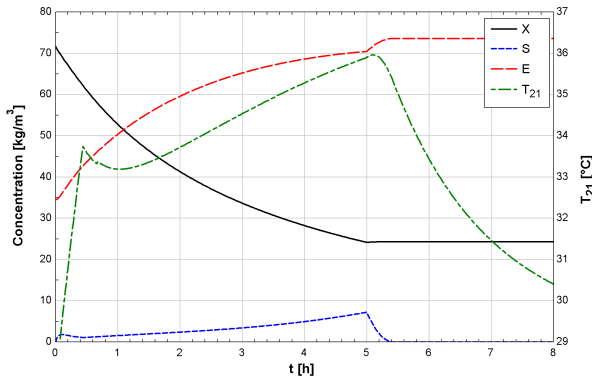


Figure 2. Ethanol E , substrate S and cell X concentration profiles for a fed-batch ethanol fermentation process using only the cooling tower to chill the vat.

For the absorption chiller and cooling tower configuration, the mass flow rate of the absorption chiller (point 18) is used to chill two fermentation vats and only half of the mass flow rate from the cooling tower is used, because some of this stream is used in the absorption chiller. As seen from Figure 3, the fermentation temperature decreases by around 1 °C with the absorption chiller/cooling tower and the final ethanol concentration is 74.17 kg m⁻³, increasing the ethanol concentration by around 0.57 kg m⁻³, which represents an annual ethanol increase of approx. 240 m³ per fermentation vat. The fermentation efficiency of process is 89.2 % and ethanol productivity is 8.0 kg m⁻³ h⁻¹, considering 8 h of fermentation.

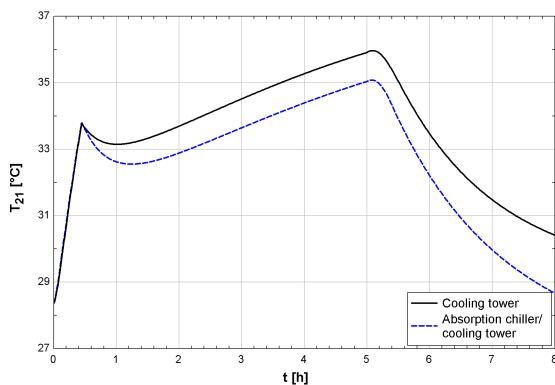


Figure 3. Fermentation temperature profiles T_{21} using the cooling tower and the absorption chiller/cooling tower.

With the cooling system shown in Figure 1, the cooling capacity of the absorption chiller is not sufficient

to remove all the heat released during the fermentation. The fermentation temperature T_{21} continues to vary and differs greatly from the ideal temperature (32 °C). A simulation with the fermentation temperature kept constant at 32 °C during the whole process was performed, and the final ethanol concentration reached 75.37 kg m⁻³, representing an annual ethanol increase of around 770 m³ per fermentation vat. In this case, the fermentation efficiency and the ethanol productivity are 90.9 % and 8.1 kg m⁻³ h⁻¹, respectively. The fermentation efficiency increased 2.5 % in comparison with that of the refrigeration system with only the cooling tower.

Thus, keeping the temperature at the ideal value can readily give several improvements in the process in terms of fermentation efficiency, productivity and cell viability. At high temperatures, the specific growth rate of contaminant microorganisms is increased, thus increasing the degree of contamination in the process. This contamination causes flocculation of the yeast cells, leading to problems in the centrifugation and incurring high costs for antibiotics. The high ethanol concentration combined with the high temperatures submits the cells to stress conditions. Under these conditions the yeast has a higher tendency to produce glycerol, which is the main by-product of ethanol fermentation. Thus, lower temperatures reduce the glycerol production, increasing the process efficiency.

Working with a lower fermentation temperature, the inlet substrate concentration S_{in} of the vat can be increased without adversely affect the fermentation process. Thus, on increasing the inlet substrate concentration, the production of ethanol in the fermentation vat increases and a wine with a higher ethanol concentration is passed to the distillery, producing a smaller amount of vinasse and requiring a lower thermal load (Camargo et al. 1990). The optimization of the fermentation process to increase the ethanol productivity, maintain cell viability and decrease the fermentation time, is needed when a higher inlet substrate concentration is used.

The heat flow released during the fermentation \dot{Q}_f and the heat flow of the fermentation heat exchanger \dot{Q}_{fhx} with the absorption chiller/cooling tower are shown in Figure 4. As seen from the figure, the heat flow of fermentation is greater than the heat flow of the heat exchanger, thus the fermentation temperature increases during the process. The ideal process would be when the heat flow released and the heat flow of the heat exchanger are the same. This can be achieved by controlling the fermentation temperature using the chilled water flow valve as the manipulated variable or using cold water with a high mass flow rate to maintain the ideal temperature.

Pressures profile of the absorption chiller internal flows is presented in Figure 5. High and low pressures increase slightly because of the temperature variation of cooling tower outlet, thereby internal temperatures are also affected, as shown in Figure 6. Chiller's COP variations during the fermentation process are negligible, holding close to 0.81.

The lithium bromide concentrations of the weak solution ξ_3 and the strong solution ξ_4 are shown in Figure 7. The concentrations and the concentration differ-

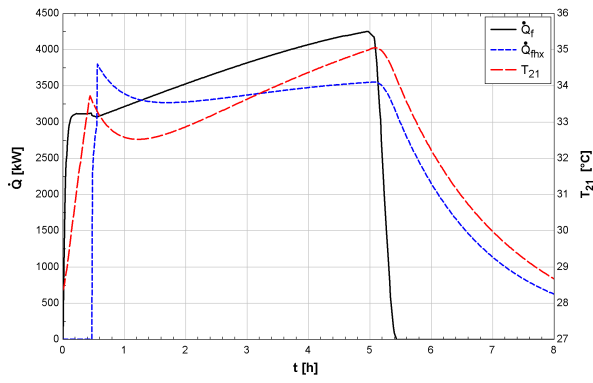


Figure 4. Heat flow rate released during ethanol fermentation \dot{Q}_f , heat flow rate of the fermentation heat exchanger \dot{Q}_{fhx} and fermentation temperature T_{21} .

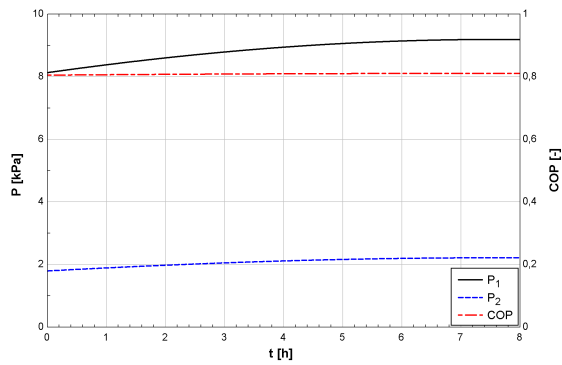


Figure 5. Pressure profile of absorption chiller internal flows.

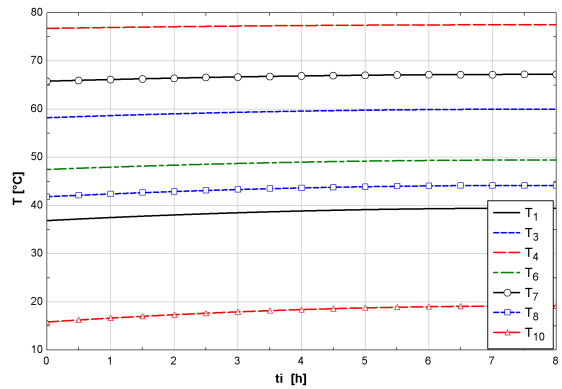


Figure 6. Temperature profile of absorption chiller internal flows.

ence $\Delta\xi$ between the strong and the weak solution decrease during the ethanol fermentation. Thus the mass flow rate of the superheated steam (point 7) decreases, and the cooling capacity \dot{Q}_e of the absorption chiller also decreases, as seen in Figure 8. The crystallization line ξ_{cryst} presented in Figure 7 shows the value of the lithium bromide mass fraction at point 6 from which the crystallization process occurs. The difference between the lithium bromide mass fraction of the strong solution ξ_4 and the mass fraction of the crystallization point ξ_{cryst} is around 10 %, showing that the operational conditions of the absorption chiller differ considerably from those

of the crystallization phenomenon.

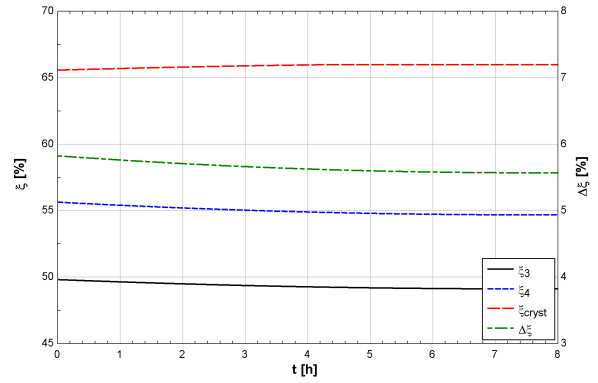


Figure 7. Variation of the lithium bromide mass fraction during the fermentation process.

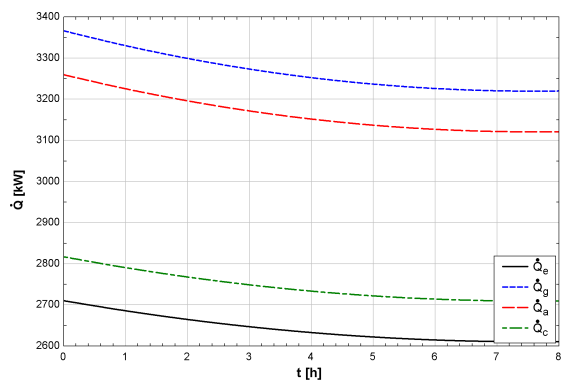


Figure 8. Heat flows variation during the fermentation process.

Similarly, the profile of the heat flow input in the absorption chiller was obtained during the fermentation process and is shown in Figure 8. The cooling capacity \dot{Q}_e decreases by around 4 % during the process. Thus, it can affect the fermentation temperature and reduce the fermentation efficiency. There are some alternatives available to increase the cooling capacity of the machine which include: increasing the water loop inlet temperature generator T_{11} or decreasing the temperature of the water from the cooling tower T_{23} that enters in the condenser T_{15} and evaporator T_{17} .

During the fermentation, the water loop outlet evaporator temperature T_{18} increases by around 3 °C, because of the temperature variation of the water from the cooling tower. The water loop outlet generator temperature T_{12} is around 88 °C. This stream can still be used in another process to improve the energy efficiency of the plant, either in a cooling capacity or to improve other processes such as air conditioning systems, sugar dryers, recovery of alcoholic gas in the distillery and cooling of must or wine.

The temperature of the water from the cooling tower T_{23} is an important parameter as it affects the performance and the cooling capacity of the absorption chiller. As seen in Figure 9, on increasing the water temperature, the heat flow input in the absorption chiller decreases. The cooling capacity \dot{Q}_e is affected by the cool-

ing tower and it is essential to keep the water temperature as low as possible. For each 1 °C increase in the temperature of the water from the cooling tower, the cooling capacity of the absorption chiller decreases by around 35 kW, which is the cause of the reduction in the cooling capacity shown in Figure 8.

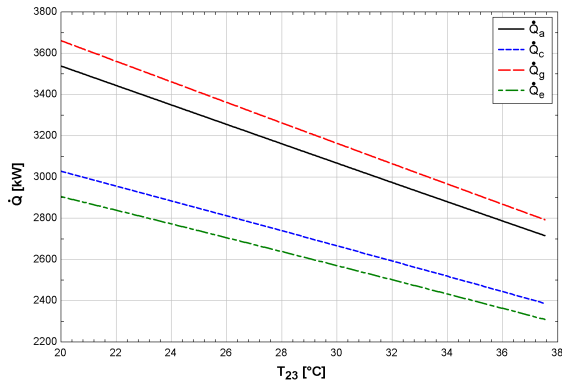


Figure 9. Heat flow input to the absorption chiller with the variation in the temperature of the water from the cooling tower.

4 Conclusions

The introduction of an absorption chiller in the ethanol fermentation cooling system has been investigated in this paper. A dynamic model for the fed-batch fermentation process coupled with a quasi-steady state model for the absorption system was developed under industrial conditions.

The simulation with the new configuration of the refrigeration system (absorption chiller and cooling tower) showed that it is possible to reduce the fermentation temperature by around 1 °C and increase the fermentation efficiency by around 0.8 %, representing an annual ethanol increase of around 240 m³ per fermentation vat. These results can be improved by decreasing the temperature to an ideal value in terms of both fermentation kinetics and cell viability. To improve these results, a refrigeration machine with a higher cooling capacity should be used, under controlled operating conditions. An increase in the ethanol concentration of the wine can reduce significantly the energy consumption in the downstream processes, such as distillation and vinasse concentration. The industrial losses, especially those related to contamination of the fermentation medium, can be minimized through a temperature control.

The results of this study demonstrate the potential application of the absorption chiller in the fermentation process. An absorption chiller powered by industrial waste heat is an excellent energy saving option in a co-generation system in a sugar and ethanol plant. This may also promote an increase in the energy balance of the ethanol production process, the value for which is currently around 8.5. All of these advantages contribute also to the competitiveness and sustainability of ethanol industry.

Acknowledgements

The authors would like to acknowledge Usina Ceradinho Açúcar e Alcool S/A for making available the

process data and the FINEP for the financial support of this study.

Nomenclature

COP	coefficient of performance
Cp	specific heat capacity, $\text{kJ kg}^{-1} \text{K}^{-1}$
E	ethanol concentration, kg m^{-3}
h	enthalpy, kJ kg^{-1}
K_i	substrate inhibition coefficient, $\text{m}^3 \text{kg}^{-1}$
K_S	substrate saturation constant, kg m^{-3}
M	molecular mass, kg kmol^{-1}
\dot{m}	mass flow rate, kg h^{-1}
m_E	ethanol production associated with growth, $\text{kg kg}^{-1} \text{h}^{-1}$
m_X	maintenance coefficient, $\text{kg kg}^{-1} \text{h}^{-1}$
n	product inhibition power
P	pressure, kPa
\dot{Q}	heat flow, kW
S	substrate concentration, kg m^{-3}
t	time, h
T	temperature, °C
UA	overall thermal conductance, kW K^{-1}
V	working volume, m^3
\dot{V}	volume flow rate, $\text{m}^3 \text{h}^{-1}$
X	cell concentration, kg m^{-3}
y	mole fraction
Y	yield factor, kg kg^{-1}
\dot{W}	power, kW

Greek symbols

ΔH_S	fermentation heat released, kJ kg^{-1}
Δt	time difference, h
η	efficiency, %
μ	specific growth rate, h^{-1}
ϕ	productivity, $\text{kg m}^{-3} \text{h}^{-1}$
ρ	density, kg m^{-3}
ξ	lithium bromide mass fraction, %

References:

- Albers, E., Larsson, C., Lidén, G., Niklasson, C., and Gustafsson, L. (2002). Continuous estimation of product concentration with calorimetry and gas analysis during anaerobic fermentations of *Saccharomyces cerevisiae*. *Thermochimica acta*, 394:185–190.
- Aldigui, A. S., Alfenore, S., Cameleyre, X., Goma, G., Uribebarrea, J. L., Guillouet, S. E., and Molina-Jouve, C. (2004). Synergistic temperature and ethanol effect on *Saccharomyces cerevisiae* dynamic behaviour in ethanol bio-fuel production. *Bioprocess and Biosystems Engineering*, 26(4):217–222.
- ASHRAE (2001). *HVAC Fundamentals Handbook*. American Society of Heating, Refrigerating and Air-Conditioning Engineers.
- Atala, D. I. P., Costa, A. C., Maciel, R., and Maugeri, F. (2001). Kinetics of ethanol fermentation with high biomass concentration considering the effect of temperature. *Applied Biochemistry and Biotechnology*, 91-93(1-9):353–365.
- Bejan, A. and Kraus, A. D. (2003). *Heat Transfer Handbook*. John Wiley and Sons, Inc.

- Camargo, C. A., Ushima, A. H., Ribeiro, A. M. M., Souza, M. E. P., and Santos, N. F. (1990). *Conservação de Energia na Indústria do Açúcar e do Alcool*. IPT - Instituto de Pesquisas Tecnológicas.
- Ghose, T. K. and Tyagi, R. D. (1979). Rapid ethanol fermentation of cellulose hydrolysate. I. Batch versus continuous systems. *Biotechnology and Bioengineering*, 21:1387–1400.
- Herold, K. E., Radermacher, R., and Klein, S. A. (1996). *Absorption Chillers and Heat Pumps*. CRC Press.
- IAPWS (1995). *Formulation for the Thermodynamic Properties of Ordinary Water Substance for General and Scientific Use*. The International Association for the Properties of Water and Steam.
- Jarzebski, A. B. and Malinowski, J. J. (1989). Modeling of ethanol fermentation at high yeast concentrations. *Biotechnology and Bioengineering*, 34:1225–1230.
- Klein, S. A. and Alvarado, F. L. (2008). *Engineering Equation Solver*, volume 8.160-3D. F-Chart Software.
- Lee, J. M., Pollard, J. F., and Coulman, G. A. (1983). Ethanol fermentation with cell recycling: computer simulation. *Biotechnology and Bioengineering*, 25:497–511.
- Patterson, M. R. and Perez-Blanco, H. (1988). Numerical fits of the properties of lithium-bromide water solutions. *ASHRAE Transactions*, 94(2):2059–2077.
- Phisalaphong, M., Srirattana, N., and Tanthapanichakoon, W. (2006). Mathematical modeling to investigate temperature effect on kinetic parameters of ethanol fermentation. *Biochemical Engineering Journal*, 28:36–43.
- Rao, J., Das, M., and Das, S. K. (2009). Changes in physical and thermo-physical properties of sugarcane, palmyra-palm and date-palm juices at different concentration of sugar. *Journal of Food Engineering*, 90:559–566.
- Torija, M. J., Rozés, N., Poblet, M., Guillamón, J. M., and Mas, A. (2003). Effects of fermentation temperature on the strain population of *Saccharomyces cerevisiae*. *International Journal of Food Microbiology*, 80:47–53.
- Yuan, Z. and Herold, K. E. (2005). Specific heat measurements on aqueous lithium bromide. *International Journal of Heating, Ventilation, Air Conditioning and Refrigerating Research*, 11(3):361–375.